Biophysical Chemistry 126 (2007) 124–131

Biophysical Chemistry

http://www.elsevier.com/locate/biophyschem

Association temperature governs structure and apparent thermodynamics of DNA–gold nanoparticles

Bernd Beermann [a], Ernesto Carrillo-Nava [b], Andy Scheffer [c], Wolfgang Buscher [c], Anup M. Jawalekar [d], Frank Seela [d], Hans-Jürgen Hinz [a,d,*]

[a] *Westfälische Wilhelms-Universität, Institut für Physikalische Chemie, Corrensstr. 30, 48149 Münster, Germany*
[b] *Laboratorio de Termofisica, Departamento de Fisicoquímica, Facultad de Química, Universidad Nacional Autónoma de México, México, D. F. 04510, México*
[c] *Westfälische Wilhelms-Universität, Institut für Anorganische und Analytische Chemie, Corrensstr. 30, 48149 Münster, Germany*
[d] *Center for Nanotechnology (CeNTech), Gievenbecker Weg 11, 48149 Münster, Germany*

Received 8 March 2006; accepted 10 May 2006
Available online 6 June 2006

Abstract

Apparent thermodynamics of association of DNA-modified gold nanoparticles has been characterized by UV spectroscopy and dynamic light scattering (DLS). Extinction coefficients of unlabelled and DNA-labelled gold nanoparticles have been determined to permit quantitative analysis of the absorption measurements. In contrast to previous studies the associating gold nanoparticles were furnished with complementary oligonucleotide DNA single strands. This resulted in direct complex formation between the nanoparticles on mixing without the requirement of a DNA linker sequence for initiation of cluster formation. Melting curves of the nanoparticle assemblies formed at different temperatures were subjected to two-state analysis. A comparison of the apparent thermodynamic parameters obtained for the dissociation of these aggregates suggests that both thermodynamically and structurally different nanoparticle clusters are obtained depending on the temperature at which assembly proceeds. The van't Hoff enthalpies permit an estimate of the DNA duplexes: gold nanoparticle ratio involved in network formation.

Keywords: Gold nanoparticles; DNA network formation; Melting curves; Extinction coefficients; Atom emission spectroscopy; Stability

1. Introduction

In recent years there has been active research in developing strategies for the controlled assembly of nanoparticles into two- and three-dimensional functional structures. Since nanoparticle assemblies exhibit collective physical and chemical properties that are significantly different from those of the individual building blocks, it is important to quantitatively characterize their structural, spectroscopic, kinetic and thermodynamic properties. Within the nanoparticles field, DNA-labelled gold particles have assumed a prominent position as a result of the versatility of network formation that is accessible through variations in base pair composition and DNA duplex length. The development of DNA-labelled gold particles has opened up a new field of nanobiotechnology [1], with applications such as the reversible switching of nanoparticle aggregation [2], nanosensors based on responsive polymer bushes [3], and the detection of single nucleotide polymorphisms (SNPs) [4].

Before optimal control over the design properties of these nanoparticles can be achieved, it is critical to determine the nature and magnitude of the driving forces involved in aggregation, as well as their kinetic and environmental determinants. The most extensively studied DNA-driven nanoparticle system is the three-DNA-strand system developed by Mirkin et al. [5]. In this system two sets of oligonucleotide-modified gold nanoparticles are coupled to form extended structures through the interaction of these nanoparticle-bound oligonucleotides with a third complementary DNA strand. This process has been shown to be reversible by raising the temperature above that of the melting temperature of the

* Corresponding author. Institut für Physikalische Chemie Corrensstr. 30 48149 Münster Germany. Tel.: +49 251 83 23427; fax: +49 251 83 29163.
E-mail address: hinz@uni-muenster.de (H.-J. Hinz).

0301-4622/$ - see front matter © 2006 Elsevier B.V. All rights reserved.
doi:10.1016/j.bpc.2006.05.020

DNA duplexes. Due to the molecular recognition properties of the DNA strands, this strategy allows one to control interparticle distance, strength of the particle interconnects, and size and chemical identity of the particles in the targeted macroscopic structure. The melting temperatures and the optical properties of the nanostructures were found to depend on salt concentration, distance between the gold nanoparticles, size of the nanoparticles, the surface density of the oligonucleotides and the concentration of the third hybridizing DNA strand [6,7]. Although many facets of the nanoparticle assembly process have been addressed by these studies, there is surprisingly little information on the thermodynamics of the individual DNA hybridization events of the DNA-labelled gold nanoparticles. Our studies have been directed towards characterizing the direct assembly of DNA-labelled gold nanoparticles in the absence of the third linking oligonucleotide single strand. Thermodynamic information was derived from quantitative analysis of melting curves following methods described previously [8].

The DNA–oligonucleotides employed in this study were 24-mers having the following sequences:

5′-d(TAGGTCAATACT TAGGTCAATACT)	**(I)**
5′-d(AGTATTGACCTA AGTATTGACCTA)	**(II)**

The oligonucleotides were coupled to the gold nanoparticles via thiol groups using the linker –O–$(CH_2)_6$–SH at the 5′-end. Both strands consist of a non self-complementary dodecamer repeat that negates the possibility of the formation of internal loops. The repetition of the dodecameric motif in the 24 mer could have a remarkable consequence for duplex formation since it offers two distinct possibilities of single strand association: (a) the interaction of all 24 bases of one strand with the complementary bases of the second strand to form a 24-mer double helix; (b) the interaction of the 3′-dodecamer of one single strand with the complementary dodecamer of the other strand to form a 12 bp duplex.

The two modes of interaction should be distinguishable by their thermodynamic parameters. The formation of a DNA–gold nanoparticle network from the association of gold particles connected by more than one type of double helix should have profound consequences for all processes that test the cooperativity of the interactions. One method is to monitor the melting of the gold–DNA network. In order to reverse the three-dimensional association process, more than one double helix per nanoparticle must be melted. Thus the cooperativity of this process will be higher than the cooperativity observed for melting of the identical double helix formed by unligated complementary single strands. The higher cooperativity should be reflected in a transition enthalpy significantly higher than that of unligated DNA.

A further parameter of nanoparticle assembly that has not received explicit attention is the temperature at which the network is formed. In addressing this issue we have shown that the association temperature has a significant influence on both the interactions and structure of the gold–DNA–nanoparticle network.

2. Experimental section

2.1. Materials

Alkanethiol oligonucleotides with sequences (**I**) or (**II**) were either attached to 19 nm (diameter) gold nanoparticles following the procedure of Storhoff et al. [9] or were employed as free oligonucleotides. The concentrations of the stock solutions of the single-stranded nucleotides were 4.09 nM (**I**) and 4.70 nM (**II**), respectively. Solutions were prepared using phosphate based buffer consisting of 10 mM Na_2HPO_4, 300 mM NaCl, pH 7.0. The free alkanethiols employed in the UV studies require a protective group to avoid disulfide bridge formation. The protective group used in the present study was 4,4′-dimethoxytrityl.

We shall refer to gold nanoparticles labelled with sequences (**I**) or (**II**) as Au(**I**) and Au(**II**).

2.2. Methods

2.2.1. Atom emission spectroscopy (AES)

A SPECTRO Ciros CCD ICP optical emission spectrometer (SPECTRO Analytical Instruments, Kleve, Germany) with axial plasma viewing was used for the determination of the gold content. A standard cross-flow nebulizer coupled to a Scott spray chamber was used as the sample introduction system. More details on the instrumental setup is available from SPECTRO [10].

The gold content of the unmodified- and oligonucleotide-modified gold nanoparticle solutions was determined via inductively coupled plasma optical emission spectrometry. This technique utilizes atmospheric argon plasma to vaporize, atomize and ionize gaseous, liquid or even solid samples. Moreover the high plasma temperatures (ca. 6000 K) cause the sample components to emit element-specific radiation. A Paschen–Runge polychromator was used to detect the radiation with a circular CCD array. For sample introduction a cross flow nebulizer coupled to a Scott spray chamber was used to create an aerosol that is transported into the plasma by the sample carrier gas flow. An external calibration method was applied. The calibration solutions were prepared by diluting a gold standard stock solution (1000 mg L^{-1}, CertiPUR, Merck KGaA) to a final concentration of 100 to 1000 μg L^{-1} with 1% hydrochloric acid (suprapur, Merck KGaA). Samples of the gold nanoparticle solutions were diluted 1 : 200 with deionised water (18.2 MΩ cm, Milli-Q Gradient, Millipore) and measured subsequently. Calibration standards and sample solutions were measured five times each with an integration time of 24 s. The gold lines observed at 201.200 nm, 242.795 nm and 267.595 nm were for single, twofold and threefold ionisation.

2.2.2. UV–Vis spectrophotometry

2.2.2.1. Determination of extinction coefficients of unlabelled and DNA-modified gold nanoparticles. UV–Vis spectra were measured using a diode array spectrophotometer (X-Dap 1024 from Axeon GmbH, Oberhausen, formerly IKS-

Optoelectronik). For the determination of the extinction coefficients of the DNA-labelled nanoparticles a dilution series (1 : 1, 1 : 2, 1 : 5, 1 : 10, 1 : 50 and 1 : 100) of the same stock solution that was employed for atom emission spectroscopy was measured in 0.1 mm, 0.2 mm, 0.5 mm, 1 mm, 5 mm and 1 cm cuvettes, respectively. The absorption measurements had an associated error of 1%.

2.2.2.2. Melting experiments. Ultraviolet melting curves were determined using self-constructed cells (d=1 cm) equipped with a Peltier temperature controller. Samples were heated from 25 to 90 °C at a rate of 1.0 K min^{-1}, while continuously monitoring the absorbance at 260 nm.

To determine the influence of the temperature at which the network was formed on the melting profiles, solutions of complementary nanoparticles labelled with the single strands (**I**) or (**II**) were mixed, each at a particle concentration of 0.28 nM. The mixtures were incubated at 7, 10, 11, 12, 13, 13.5, 14, 20, and 25 °C for 3 h. The nanoparticles remained in solution during the incubation time and the subsequent melting studies. Melting studies on the unlabelled oligonucleotide duplexes were performed using a final duplex concentration of 393 nM.

2.2.3. Quantification of the average covering of the gold nanoparticles by alkanethiol oligonucleotides

Following the procedure reported by Demers et al. [11], 0.7 μL of mercaptoethanol was added to 400 μL of a 2.98 nM (particles) solution of gold nanoparticles labelled with sequence (**II**) to obtain a final concentration of 24 mM. After 18 h of shaking at room temperature, the gold was separated from the solution containing the displaced oligonucleotides by centrifugation (8000 rpm; Sigma 3 K30 centrifuge, Brown Biotech Int., Melsungen, Germany; Eppendorf 1.5 mL cups). The oligonucleotide concentration was determined by measuring the absorbance of the supernatant at 260 nm (ε=243 000 M^{-1} cm^{-1}). The number of oligonucleotide chains per gold nanoparticle was calculated using the particle number and the known volume (400.7 μL).

2.2.4. Dynamic light scattering (DLS)

DLS measurements were performed using a DynaPro dynamic light scattering system equipped with a temperature controlled micro sampler (Protein Solutions, Charlottesville, VA, USA). DLS measurements were made on both labelled and unlabelled gold nanoparticles. The nanoparticles Au(**I**) and Au(**II**) were measured separately at 20 °C and at 5 °C using nanoparticle concentrations of 66.7 pM and 76.6 pM, respectively. Measurements were also made on solutions of a mixture of nanoparticles (cAu(**I**)=33.3 pM and cAu(**II**)= 38.3 pM). The mixtures were incubated at 20 °C for 3 h and at 5 °C for 4 h followed by DLS measurements at these incubation temperatures.

2.2.5. Data analysis

2.2.5.1. Melting curves. The melting of simple short oligonucleotide duplexes is generally described by an all-or-none dissociation reaction given in Eq. (1). This model takes into account the dependence of the equilibrium constant on concentration. DNA-labelled gold nanoparticles, on the other hand, are constructs of one gold nanoparticle labelled with n DNA–oligonucleotides, where n assumes values in the region of 200 to 400 chains depending on the surface of the gold nanoparticle. However, the formation of the gold nanoparticle–DNA network involves only a few of these attached oligonucleotides as a result of both steric effects and the curvature of the nanoparticles.

To describe DNA dehybridization within the assembly we adopt a simple two-state model. The observed sharp melting transition of the DNA–nanoparticle network suggests the presence of a small number of DNA duplex links between each pair of nanoparticles.

In a simple two-state model, the dissociation of a DNA double helix into its complementary strands is described by Eq. (1):

$$(\mathrm{DS}) \Leftrightarrow (\mathrm{SS})_1 + (\mathrm{SS})_2 \tag{1}$$

The variation with temperature of the standard Gibbs energy change of melting, ΔG^0, for heterodimers is then:

$$\Delta G^0(T) = \Delta H^0_{\mathrm{vH}}(T_\mathrm{m})\cdot\left(1-\frac{T}{T_\mathrm{m}}\right) + \Delta C_\mathrm{p}(T_\mathrm{m})\cdot\left(T - T_\mathrm{m} - T\cdot\ln\frac{T}{T_\mathrm{m}}\right) - RT_\mathrm{m}\cdot\ln\frac{c_\mathrm{t}}{4} \tag{2}$$

where c_t is the total concentration of nanoparticles labelled with single strands of any sequence, $\Delta H^0_{\mathrm{vH}}(T_\mathrm{m})$ is the van't Hoff enthalpy of double helix dissociation per mole of cooperative units at the transition temperature, T_m, and $\Delta C^0_\mathrm{p}(T_\mathrm{m})$ is the difference between the heat capacities of the single and double strand states. In order to extract the thermodynamic parameters from the UV–melting curves, the observed absorption, E_exp, is expressed as a linear combination of the extinction coefficients of the single and double strand species, E_SS and E_DS, weighted by their respective fractions, α_SS and $(1-\alpha_\mathrm{SS})$:

$$E_\mathrm{exp}(T) = E_\mathrm{SS}(T)\cdot\alpha_\mathrm{SS}(T) + E_\mathrm{DS}(T)\cdot(1-\alpha_\mathrm{SS}(T)) \tag{3}$$

The extinction coefficients of the single strands were determined experimentally at 25 °C (298 K). The extinction coefficient of the double strands were calculated from the mean of the extinction coefficients of the two single strands weighted by a correction factor, $(1-f_\mathrm{hyp})$, which takes into account the effect of hypochromicity. The parameter f_hyp is defined as the fractional decrease in absorption on duplex formation. The temperature dependences of the UV signals of the pure duplex and single strands were taken into account by linear regression analyses. A slope m_DS was assigned to the double strands, and m_SS to the single strands. The temperature dependence of the mean extinction of the single strand, $E_\mathrm{SS}(T)$, is then given by Eq. (4),

$$E_\mathrm{SS}(T) = \bar{\varepsilon}(298\ \mathrm{K})\cdot c_\mathrm{t} + m_\mathrm{SS}\cdot(T - 298\ \mathrm{K}) \tag{4}$$

and that of the double strand by Eq. (5):

$$E_{DS}(T) = \bar{\varepsilon}(298\ \mathrm{K}) \cdot (1 - f_{hyp}) \cdot \frac{c_t}{2} + m_{DS} \cdot (T - 298\ \mathrm{K}) \quad (5)$$

where $\bar{\varepsilon}$ is the mean of the extinction coefficients of the two single strands. For the analysis of the melting profiles it is assumed that at 25 °C, i.e. far below the transition temperature, complete network formation is obtained after 3 h.

The fraction of free single-stranded nanoparticles ($\alpha_{ss}(T)$) is obtained from Eqs. (6) and (7):

$$K(T) = \frac{2\alpha_{SS} c_t}{(1 - \alpha_{SS})} \quad (6)$$

$$\alpha_{SS}(T) = -\frac{K(T)}{c_t} + \sqrt{\left(\frac{K(T)}{c_t}\right)^2 + \frac{2K(T)}{c_t}} \quad (7)$$

where $K(T)$ is the apparent equilibrium constant and c_t is the total concentration of single strands.

For a fit of a UV melting curve a total of six parameters are required: T_m, ΔH^0_{vH}, ΔC^0_p, m_{SS}, m_{DS} and fhyp. However, three parameters, T_m, m_{SS} and m_{DS}, can be estimated independently of the fit. This reduces the number of necessary fit parameters to three.

3. Results and discussion

Fig. 1A gives a realistic illustration of the steric situation on the surface of the 19 nm gold nanoparticles used in the present studies. The correct proportions of the relative sizes of the gold particle and the single-stranded oligonucleotides are visualized as well as surface covering.

Upon assembly of a nanoparticle network, only a few of the multitude of single strand oligonucleotides covering each gold nanoparticle will form a duplex with a complementary single strand of the neighbouring gold particle. The following considerations provide a simplified but very helpful estimate of the number involved. If one assumes hexagonal tight packing of the nano-spheres, the maximal number of nearest neighbours is 12, of which 6 must provide the complementary sequence to render duplex formation possible. Six is likely an upper estimate of the number of duplexes that can be formed between one sphere and its next nearest neighbours given that the curvature of the nano-spheres and variation in surface coverage of oligonucleotides on individual gold particles can result in off-register duplex formation between the 24-mers. It is perhaps more realistic that a smaller number of duplexes will be formed between the nanoparticles since ideal hexagonal tight packing is not likely to occur in solution.

These arguments suggest that for the analysis of the melting of the DNA–gold nanoparticle network it is more appropriate to consider the concentration of the nanoparticles rather than the concentration of the DNA–oligonucleotides.

Although DNA-labelled gold nanoparticles appear to be much more complex systems than simple DNA duplexes, the stability of associated nanoparticles is essentially determined by the stability of the DNA duplexes formed between the nanoparticles. Thus, in principle, the overall transition enthalpy involved in the cooperative melting of the nanoparticle assembly should be approximated by an n-fold ΔH^0_{vH} value of the free DNA oligonucleotide duplex, where n is the average number of DNA duplexes dissociated per gold nanoparticle and ΔH^0_{vH} is the van't Hoff enthalpy of the dissociation of unlabelled DNA duplex (per mol of duplex).

In order to determine duplex stability using Eq. (2) it is necessary to define the concentration of nanoparticles. We determined extinction coefficients at 524 nm and 260 nm for both labelled and unlabelled gold nanoparticles. This procedure is necessary because the well established incremental approach used to estimate extinction coefficients of free DNA cannot be applied to these systems where static light scattering of the nanoparticles has a significant effect on the duplex extinction at 260 nm.

3.1. Characterization of nanoparticles

It has been shown that the extinction coefficients of unlabelled gold nanoparticles depend strongly on the size of

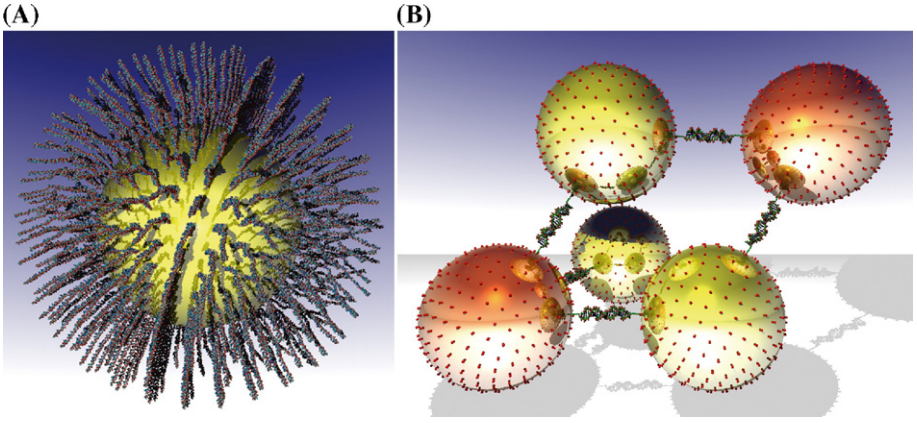

Fig. 1. Realistic views of single and assembled DNA–gold nanoparticles. The dimensions are drawn to scale. (A) Representation of a 19 nm gold nanoparticle labelled with 285 single-strand 24-mer DNA–oligonucleotides. (B) View of an ideal three-dimensional network (hexagonal packing) formed by DNA-labelled gold nanoparticles. For clarity the positions of the single strands are only indicated by red dots. The different colours of the particles indicate the different DNA labels (**I**) or (**II**).

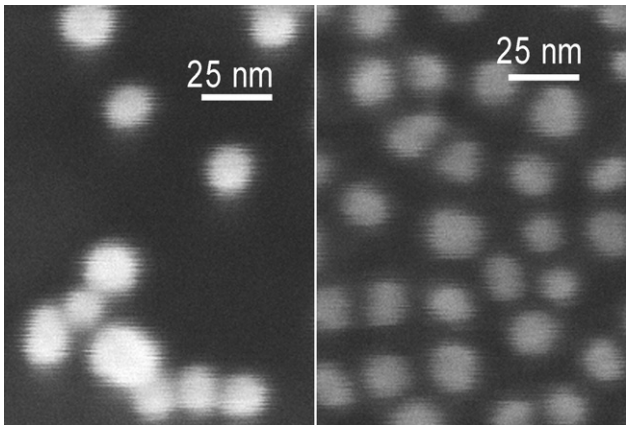

Fig. 2. SEM pictures of the unlabelled gold nanoparticles (left) and of particles labelled with sequence (**I**) (right). The average diameter is 19 nm±2 nm.

the particles [7,8]. Thus values of extinction coefficients are only useful in conjunction with values for the size of the nanoparticles. Diameters of the labelled and unlabelled gold nanoparticles were measured by scanning electron microscopy, and hydrodynamic radii were determined by DLS. The typical oligonucleotide surface coverage on the gold nanoparticles was determined for Au(**II**) by quantitative reductive detachment of the DNA and assumed to be equivalent for the Au(**I**) nano particles.

3.1.1. Determination of the extinction coefficient, diameter and hydrodynamic radius of unlabelled gold nanoparticles

Scanning electron microscopy showed that the gold nanoparticles had an average diameter of 19 nm (Fig. 2).

The average mass of one gold nanoparticle was determined to be 6.94×10^{-17} g using the density of gold (19.32 kg/L) and assuming a spherical shape of the particle. A solution of these nanoparticles exhibited an absorbance of 0.991 at 524 nm in a 1 cm cuvette. Using a value of 51± 2 μg/mL for the gold concentration determined from AES measurements a molar concentration of gold nanoparticles can be calculated as 1.70 nM. From this one obtains a molar extinction coefficient for the gold nanoparticles of 8.12×10^{8} M^{-1} cm^{-1}.

From dynamic light scattering measurements at 20 °C, the hydrodynamic radius was determined to be 10.4±2.7 nm. This value is within error identical to that determined by SEM.

3.1.2. Determination of the extinction coefficient and hydrodynamic radius of ssDNA-labelled gold nanoparticles

Solutions of gold nanoparticles labelled with sequence (**I**) exhibited an absorbance of 0.386±0.001 at 524 nm in a 1 mm cuvette. The gold concentration was determined to be 162± 8 μg/mL by AES.

Assuming an average mass of a gold nanoparticle to be 6.94×10^{-17} g, this corresponds to a molar concentration of nanoparticles of 3.88×10^{-9} M and a molar extinction coefficient of $9.96\pm0.1\times10^{8}$ M^{-1} cm^{-1} at 524 nm and $10.2\pm0.1\times10^{8}$ M^{-1} cm^{-1} at 260 nm. The corresponding values for particles labelled with sequence (**II**) are: $\varepsilon_{524}=9.95\times10^{8}$ M^{-1} cm^{-1} and $\varepsilon_{260}=10.2\times10^{8}$ M^{-1} cm^{-1}.

These data provide the basis for the calculation of thermodynamic parameters from melting curves of DNA-labelled gold nanoparticles using Eqs. (2)–(7).

From dynamic light scattering measurements, a hydrodynamic radius of 13.4±3.4 nm was determined for the gold nanoparticles labelled with sequence (**I**) and a value of 15.8± 2.2 nm for Au (**II**). The hydrodynamic radii of the labelled nanoparticles are only slightly larger than those of the unlabelled gold particles. Thus, it appears that the DNA single strands attached to the surface do not contribute to the hydrodynamic radius in proportion to their length.

A summary of extinction coefficients and radii is given in Table 1.

3.1.3. Covering of the gold nanoparticles by oligonucleotides

The number of DNA–oligonucleotides attached to one nanoparticle is a factor that could influence the stability of the gold DNA network. Following the procedure outlined in Section 2.2.3, the concentration of oligonucleotide was determined to be 0.85 μM DNA after decoupling of 400 μL of a 2.98 nM solution of gold nanoparticles labelled with sequence (**II**). This corresponds to an average surface coverage of 284 DNA strands per gold nanoparticle. Our experimental value is smaller than that reported by Petrovykh [12] for plain gold surfaces. In that study an average space requirement of 2.7 nm^2 per DNA chain was observed, which corresponds to a 19 nm gold nanoparticle with a surface area of 1134 nm^2 carrying 420 single strands.

3.2. Melting of gold–DNA aggregates

Melting profiles of DNA duplexes have been a reliable source for the determination of van't Hoff enthalpies. Short oligonucleotides have been found to exhibit high cooperativity compatible with a two-state mechanism. Melting of the 24-mer duplex (Fig. 3) results in a melting enthalpy of $\Delta H_{vH}=768$ kJ/mol at $T_m=64.5$ °C.

The UV melting curves for the denaturation of DNA–gold nanoparticle assemblies are presented in Fig. 4 and apparent thermodynamic parameters are summarised in Table 2.

Several features of the melting curves deserve comment. Significant differences are apparent in the melting profiles of assemblies formed at different annealing temperatures. Nanoparticle networks annealed at 11 °C exhibit a broader melting

Table 1
Properties of gold nanoparticles

Species	SEM radius (nm)	Hydrodynamic radius (nm)	ε(260 nm) (M^{-1} cm^{-1})	ε(524 nm) (M^{-1} cm^{-1})
(**I**)			2.41×10^{5}	
(**II**)			2.43×10^{5}	
Au	9.5	10.4±2.7		8.12×10^{8}
Au(**I**)		15.8±2.2	10.2×10^{8}	9.96×10^{8}
Au(**II**)		13.4±3.4	10.2×10^{8}	9.95×10^{8}

(**I**) and (**II**) refer to the complementary single strands. Unlabelled gold nanoparticles are referred to as Au, and gold particles labelled with (**I**) or (**II**) as Au (**I**) or Au (**II**). All molar extinction coefficients are given per mol of gold nanoparticles.

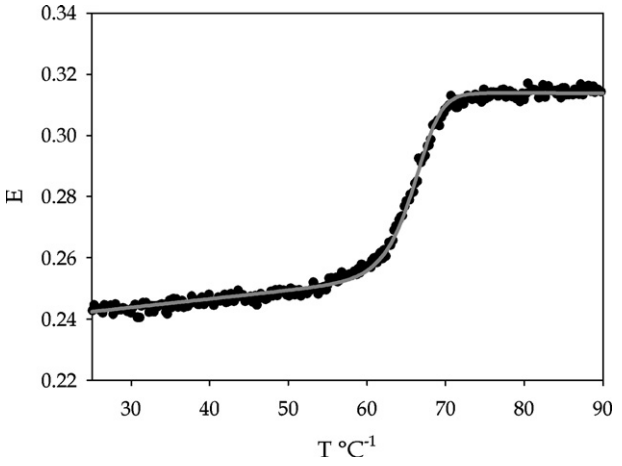

Fig. 3. UV melting curves for the denaturation of duplex DNA formed from unlabelled oligonucleotides. Measurements were carried out after incubating the samples for 6 h at RT in 10 mM sodium phosphate buffer, pH 7.0, 300 mM NaCl. The heating rate was 1 K/min.

profile compared with those annealed at higher temperatures. This qualitative observation is supported by the quantitative analysis of the melting curves.

Inspection of Table 3 reveals that melting of the nanoparticle network prepared at 11 °C is characterized by a van't Hoff enthalpy of approximately 700 kJ/mol of cooperative unit, while the networks prepared at 13.5 °C, 14 °C and 25 °C are characterized by enthalpies of 1000 kJ/mol, 2300 kJ/mol and 2800 kJ/mol, respectively. In contrast to the increase observed for the van't Hoff enthalpies, the transition temperatures

Table 2
Optical data for unligated duplex DNA and DNA–gold nanoparticle assemblies

Complexes formed [association temperature]	Degree of hypochromicity, f_{hyp} (extrapolated to 25 °C)
(**I**)+(**II**) [22 °C]	0.19±0.02
Au(**I**)+Au(**II**) [13.5 °C]	0.13±0.02
Au(**I**)+Au(**II**) [14 °C]	0.24±0.02

(**I**) and (**II**) refer to the complementary single strands, gold particles labelled with these ssDNA are referred to as Au(**I**) or Au(**II**).

decrease from 75.3 °C for an annealing temperature of 11 °C to 72.2 °C when annealed at 25 °C. However, the most remarkable feature of network melting is the observation of a doubling of ΔH_{vH} for networks prepared at 14 °C compared to those prepared at 13.5 °C. At present these observations cannot be rationalised mechanistically.

However, if we accept the ΔH_{vH} values as empirical parameters that reflect the size of the cooperative unit involved in the melting process of the three-dimensional DNA–gold nanoparticle network, one can make the following argument. With increasing association temperature the average number of DNA duplexes formed between the gold nanoparticles increases concomitant with an increase in the degree of order of the network.

The network could be viewed as a kind of crystal with varying degrees of local order, which would determine the cooperativity of melting. Both an increase in the number of interacting DNA double helices on each gold particle and/or an increase in the stability of a double helix would result in an increase in the van't Hoff enthalpy of melting. As the sequence

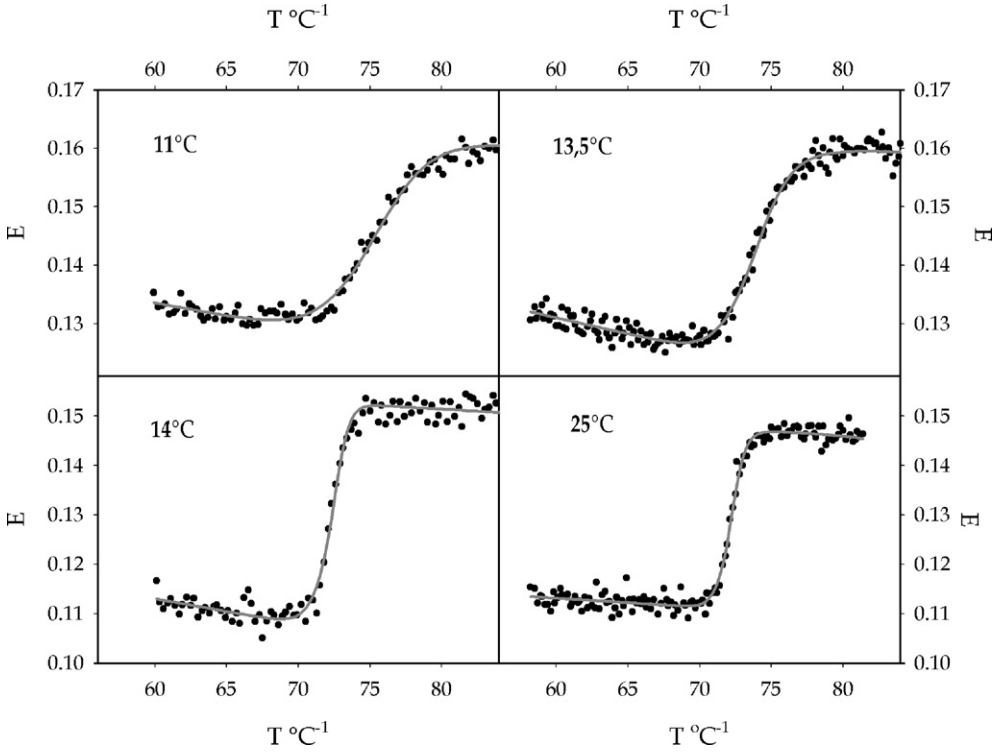

Fig. 4. UV melting curves for the denaturation of DNA–gold nanoparticle assemblies formed after annealing at 11, 13.5, 14, and 25 °C for 3 h. Samples were in 10 mM sodium phosphate buffer, pH 7.0, 300 mM NaCl. The heating rate was 1 K/min.

Table 3
Apparent thermodynamic data for the DNA–gold nanoparticle assemblies prepared at various association temperatures

$T_{assoc.}$ (°C)	T_m (°C)	ΔH^0_{vH} (kJ/mol)	ΔG^0 (25 °C) (kJ/mol)
11	75.4	679±140	398±80
12	74.9	935±190	552±110
13	74.6	975±195	663±130
13.5	73.8	1074±215	661±130
14	72.3	2295±460	878±180
15	72.6	2065±420	1497±300
25	72.1	2812±450	2140±450

employed in the present study can form either 12 or 24 bp duplexes, but no other duplexes, the approximate doubling of ΔH_{vH} when the annealing temperature was increased from 13 °C to 14 °C could be interpreted as an indication of a change in the mode of interaction between the complementary sequences of the gold particles. Although we cannot offer an explanation why this should occur in such a small temperature range, it appears plausible that, once a dodecameric duplex is formed, the activation energy required for this duplex to dissociate to allow the formation of a 24 mer duplex would be too high at the low temperature. Furthermore, the local concentration of complementary DNA single strands is significant (about 0.04 M), which would disfavour dissociation of the duplex.

The three-dimensional interactions inferred from the analysis of the melting studies and packing considerations are visualised in Fig. 1B. All dimensions are drawn to scale. We described earlier that Fig. 1A provides a realistic picture of the surface density of the DNA single strands on the gold nanoparticles. The surface properties of the nanoparticles will have a significant influence on the mechanism of cluster formation. It is possible to envisage that nanoparticle association could occur via either reaction-limited aggregation, if the repulsive barrier between the particles was dominant, or by diffusion-limited aggregation in the absence of a barrier [13]. It is not possible to infer any mechanistic details from the present studies; however, consideration of the packing constraints together with the van't Hoff enthalpies for cluster dissociation permit some more specific comments on the nature of the nanoparticle assemblies. We have described earlier that assuming a random distribution of the complementary nanoparticles within a hexagonal tight packing arrangement of the network it would be possible to form 6 duplexes between one sphere and its nearest neighbours. As each bond is shared by two nanoparticles the average number of bonding interactions per particle would be 3. If the "bond" between the nanoparticles is given by "one double helix", cooperative melting of these bonds would be associated with 3 times the van't Hoff enthalpy of a single oligonucleotide double helix. Since we have determined the van't Hoff enthalpy for cooperative melting of unlabelled DNA, it is possible to estimate the number of cooperatively melting DNA sequences associated with melting of the network by comparing the corresponding enthalpy values. Using an average van't Hoff enthalpy of 2500±400 kJ/mol per cooperative unit for melting of the network prepared at annealing temperature of between 14 and 25 °C and ΔH_{vH}=750±60 kJ/mol for unlabelled duplex

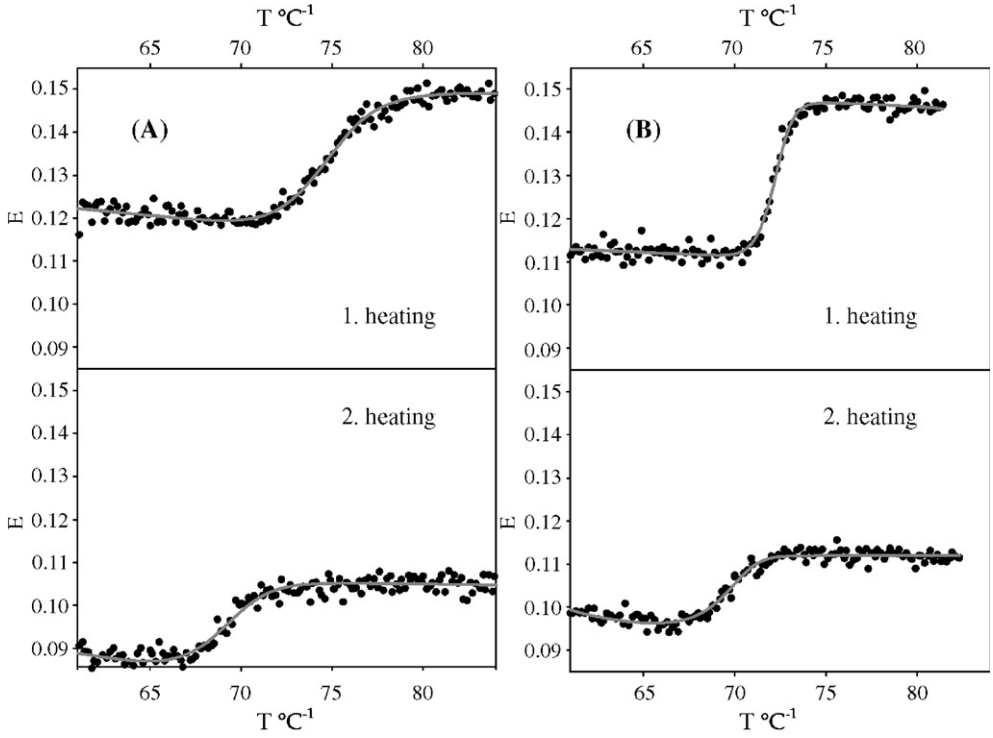

Fig. 5. Reversibility tests: Melting of DNA–gold nanoparticle assemblies prepared at 13 °C (A) and at 25 °C (B). Samples were in 10 mM sodium phosphate buffer, pH 7.0, 300 mM NaCl. Heating rate was 1 K/min. The second heating was performed after cooling to 60 °C with a cooling rate of 0.25 K/min and annealing at this temperature for 1 h. The melting was monitored at 524 nm. (A) First heating: T_m=74.7 °C, ΔH^0_{vH}=974 kJ/mol; second heating: T_m=69.0 °C, ΔH^0_{vH}=1074 kJ/mol. (B) First heating: T_m=72.2 °C, ΔH^0_{vH}=2812 kJ/mol; second heating: T_m=69.1 °C, ΔH^0_{vH}=1117 kJ/mol. The reported enthalpies are per mol of cooperative unit.

melting, the number of cooperatively melting duplexes is approximately 3 to 4. This relatively small average number of bonds can account for the increase in stability and cooperativity of melting of the DNA–gold nanoparticle assembly compared to that of free DNA duplexes. This situation is illustrated in Fig. 1B. The red particle on the left binds to three yellow binding partners on its right side and would have three equivalent yellow spheres on the left side. For clarity the single strand positions on the gold surface are represented only by dots.

Reversibility of network formation was investigated for nanoparticle assemblies prepared at annealing temperatures of 13 °C and 25 °C by repeated melting of the samples after cooling to 60 °C at a rate of 0.25 K/min followed by an incubation time of 60 min. The results are illustrated in Fig. 5.

Nanoparticle assemblies prepared at 13 °C exhibit on second heating transition curves with a similar van't Hoff enthalpy of approximately 1000 kJ/mol of cooperative unit. However, re-melting is characterized by a lower T_m value and a smaller hyperchromic effect. These observations can be rationalised in the following manner. It is well known that part of the highly polymerized network can irreversibly precipitate over the duration of the experiment. This would be observed as a decrease in the initial and final absorption values, in accordance with the experimental observations. The nanoparticle assembly remaining in solution melts with the same cooperativity as the original sample. The observed shift to lower transition temperature would be a consequence of the lower total concentration of nanoparticles. The analogous studies on nanoparticle assemblies prepared at 25 °C show an interesting difference. Here re-melting of the assembly does not exhibit the same high cooperativity as the first melting but a lower cooperativity similar to that observed for the assembly prepared at 13 °C. This suggests that the incubation conditions were not sufficient to reproduce the nanoparticle network originally formed at 25 °C.

3.3. Summary

Apparent thermodynamic parameters derived from melting studies are an appropriate method for the characterization of DNA–gold nanoparticle assemblies. Our studies have shown that the melting of the assembly is characterized by a larger van't Hoff enthalpy compared to that of free duplex DNA concomitant with an increase of the cooperative unit of DNA melting. A somewhat different interpretation was provided by Park and Stroud [13]. They also make the assumption that multiple duplexes exist between the nanoparticles but in their analysis the melting of these duplexes is not considered to be cooperative. In their studies, the narrowing of the melting interval is described by a model in which the melting of each duplex is characterized by a probability function that is defined by the number of DNA strands present per pair of gold nano particles. The present studies do not allow us to differentiate between this model and the cooperative model we propose.

Acknowledgements

E. C.-N. thanks Deutscher Akademischer Auslandsdienst (DAAD) and Universidad Nacional Autónoma de México (UNAM) for financial support. We are grateful to J. Guddorf for excellent technical assistance and acknowledge the participation of K. Brinckmann, B. Hasken, T. Kleine, T. Kösterke, E. Krämer, and R. Seyer in parts of the present study. We thank J. Chaires and N. Garbett for the removal of Germanisms from the paper and for the improvement of readability.

References

[1] J.J. Storhoff, C.A. Mirkin, Programmed materials synthesis with DNA, Chem. Rev. 99 (1999) 1849–1862.
[2] C.M. Niemeyer, C.A. Mirkin, NanoBiotechnology. Concepts, Methods, Applications, Wiley-VCH, Weinheim, 2004.
[3] P. Hazakira, B. Ceyhan, C.M. Niemeyer, Reversible switching of DNA–gold nanoparticle aggregation, Angew. Chem., Int. Ed. 43 (2004) 6469–6471.
[4] I. Tokareva, S. Minko, J.H. Fendler, E. Hutter, Nanosensors based on responsive polymer brushes and gold nanoparticle enhanced transmission surface plasmon resonance spectroscopy, J. Am. Chem. Soc. 126 (2004) 15950–15951.
[5] T. Ihara, S. Tanaka, Y. Chikaura, A. Jyo, Preparation of DNA-modified nanoparticles and preliminary study for colorimetric SNP analysis using their selective aggregations, Nucleic Acids Res. 32 (2004) e105.
[6] C.A. Mirkin, R.L. Letsinger, R.C. Mucic, J.J. Storhoff, A DNA-based method for rationally assembling nanoparticles into macroscopic materials, Nature 382 (1996) 607–609.
[7] J.J. Storhoff, A.A. Lazarides, R.C. Mucic, C.A. Mirkin, R.L. Letsinger, G.C. Schatz, What controls the optical properties of DNA-linked gold nanoparticle assemblies, J. Am. Chem. Soc. 122 (2000) 4640–4650.
[8] A.K.R. Lytton-Jean, C.A. Mirkin, A thermodynamic investigation into the binding properties of DNA functionalized gold nanoparticle probes and molecular fluorophore probes, J. Am. Chem. Soc. 127 (2005) 12754–12755.
[9] J.J. Storhoff, R. Elghanian, R.C. Mucic, C.A. Mirkin, R.L. Letsinger, One-pot colorimetric differentiation of polynucleotides with single base imperfections using gold nanoparticle probes, J. Am. Chem. Soc. 120 (1998) 1959–1964.
[10] SPECTRO, ICP-report, no. ICP-17, (2001) SPECTRO Analytical Instruments, Kleve.
[11] L.M. Demers, C.A. Mirkin, R.C. Mucic, R.A. Reynolds III, R.L. Letsinger, R. Elghanian, G. Viswanadham, A fluorescence-based method for determining the surface coverage and hybridization efficiency of thiol-capped oligonucleotides bound to gold thin films and nanoparticles, Anal. Chem. 72 (2000) 5535–5541.
[12] D.Y. Petrovykh, H. Kimura-Suda, L.J. Whitman, M.J. Tarlov, Quantitative analysis and characterization of DNA immobilized on gold, J. Am. Chem. Soc. 125 (2003) 5219–5226.
[13] S.Y. Park, D. Stroud, Structure formation, melting, and optical properties of gold/DNA nanocomposites: effects on relaxation time, Phys. Rev., B 68 (2003) 224201-1–224201-11.